

Spectroscopic Temperature Determination of Degenerate Fermi Gases

Marijan Koštrun and Robin Côté

Physics Department, University of Connecticut, 2152 Hillside Rd., Storrs, Connecticut 06269-3046.

(Dated: November 14, 2018)

We suggest a simple method for measuring the temperature of ultra-cold gases made of fermions. We show that by using a two-photon Raman probe, it is possible to obtain lineshapes which reveal properties of the degenerate sample, notably its temperature T . The proposed method could be used with identical fermions in different hyperfine states interacting via s -wave scattering or identical fermions in the same hyperfine state via p -wave scattering. We illustrate the applicability of the method in realistic conditions for ${}^6\text{Li}$ prepared in two different hyperfine states. We find that temperatures down to $0.05 T_F$ can be determined by this *in-situ* method.

PACS numbers:

I. INTRODUCTION

The experimental realization of Bose-Einstein condensation (BEC) in atomic samples [1] have stimulated a new wave of theoretical and experimental studies of degenerate systems in the dilute and weakly interacting regime. Several recent experiments have successfully reached the degenerate regime for ultra-cold atomic samples of fermions. For example, temperatures of $0.5 T_F$ or less, where T_F is the Fermi temperature of the cold fermions, have been reported for ${}^{40}\text{K}$ [2], or ${}^6\text{Li}$ [3]. One of the goals of reaching even lower temperatures is the formation of Cooper pairs of interacting fermions and the detection of the Bardeen-Cooper-Schrieffer (BCS) phase transition in a trapped gas of fermionic atoms. Such transitions in atomic gases will allow the study of phenomena usually associated with condensed matter physics, such as superconductivity. Recently, “resonance superfluidity” [4] has been predicted in the strong-coupling regime occurring near a Feshbach resonance. This regime is being explored experimentally [5].

One of the key parameters in studying these systems is the accurate value of the temperature T . Various methods are being employed to determine T , such as fitting the tail of the fermion energy distribution [6], using mixtures with bosons [3], or using impurities as probes [7]. Each of these approaches have limitations. For example, considering that the thermal contribution in a Fermi gas vanishes with temperature, fitting the tail of the energy distribution becomes very challenging. Even in a fermion-boson mixture with large attractive interactions, such as ${}^{40}\text{K}$ - ${}^{87}\text{Rb}$ [8, 9], or ${}^6\text{Li}$ - ${}^7\text{Li}$ [3], it is questionable whether bosons and fermions stay in thermal equilibrium when the temperature is lowered to degenerate regime. Even if so, the determination of the bosons temperature is not easy below $T_c/2$ (T_c : BEC critical temperature) [10]. Typically, temperature is read by imaging the velocity distribution of a freely expanded sample.

In this paper, we describe an *in situ* method to measure the temperature of a sample based on spectroscopic measurements. It offers the potential for very accurate determination of extremely low temperatures in degenerate Fermi systems as well as other properties (e.g., their

Fermi temperature T_F). Furthermore, if used in systems made of fermions only, it avoids the problem arising from the superfluidity of Bose-Einstein condensates when T is below the BEC critical temperature T_c , which suppresses scattering [11]. The approach is based on Doppler-free two-color spectroscopy. Such techniques have been successfully employed to create ultra-cold dimers in ultra-cold bosonic gases and in BEC [12].

II. METHOD

The schematic of the two-photon transition is illustrated in Fig. 1, together with the relevant quantities. While two atoms approach each other along the molecular ground state with a given relative kinetic energy ϵ , two co-propagating lasers can induce a two-photon transition into a bound level E_{b2} of the molecular ground state. The first laser of intensity I_1 is detuned from the excited molecular bound level E_{b1} by $\delta_1 = E_{b1} - \nu_1$. Similarly, the second laser of intensity I_2 is detuned by an amount $\delta_2 = E_{b2} - (\nu_1 - \nu_2)$ from the bound level energy E_{b2} of the ground molecular state. The rate coefficient for the photoassociation (PA) process is given by [13]

$$\mathcal{K}(T, L_1, L_2) = \left\langle \frac{\pi v}{\kappa^2} \sum_l (2l+1) |S_l(\epsilon, L_1, L_2)|^2 \right\rangle, \quad (1)$$

where $L_i = \{I_i, \delta_i\}$ represent the parameters of laser i , $\epsilon = \hbar^2 \kappa^2 / 2\mu = \mu v^2 / 2$, μ is the reduced mass, and v is the relative velocity of the colliding pair. In Eq.(1) the sum goes over contributing partial waves l , and S_l represents the scattering matrix element for producing the final state E_{b2} from the initial continuum state. Averaging over relative velocities is implied by $\langle \dots \rangle$. The scattering matrix is well approximated by [13]

$$|S_l|^2 = \frac{(\epsilon - \delta_2)^2 \gamma_1 \gamma_s}{(\epsilon - \Delta_+)^2 (\epsilon - \Delta_-)^2 + (\gamma^2/4)(\epsilon - \delta_2)^2}, \quad (2)$$

where γ_1 is the width of the intermediate bound level E_{b1} and $\gamma_s \simeq 4\pi^2 (I_1/c) |\langle E_{b1} | D(R) | \epsilon, l \rangle|^2$ is the stimulated width from the continuum initial state $|\epsilon, l\rangle$ to the

intermediate state $|E_{b1}\rangle$. Here, $D(R)$ is the molecular dipole transition moment, and in the zero-energy limit, $\gamma_s \propto \epsilon^{1/2+l}$. Also, $\gamma = \gamma_1 + \gamma_s \simeq \gamma_1$ if the laser intensities are not too large (this is the regime we are interested in). Finally, Δ_{\pm} represent a split in the single resonance due to the second laser, and is given by

$$\Delta_{\pm} = \frac{1}{2}(\delta_1 + \delta_2) \pm \frac{1}{2}\sqrt{(\delta_1 - \delta_2)^2 + 4h^2\Omega_2^2}, \quad (3)$$

where $h^2\Omega_2^2 = (2\pi I_2/c)|\langle E_{b1}|D(R)|E_{b2}\rangle|^2$ defines the Rabi frequency Ω_2 . From the analytical form of $|S_l|^2$, we expect two peaks located at $\epsilon \simeq \Delta_{\pm}$, and a minimum ($|S_l|^2 = 0$) located between the peaks at $\epsilon = \delta_2$ (due to destructive interference between the two scattering paths). Because of the $\epsilon^{1/2+l}$ Wigner's threshold behavior of γ_s , the peak at Δ_- will be weaker than the one at Δ_+ .

We consider samples of identical fermions of mass m in the ultra-cold regime (so that $2\mu = m$). While there is no s -wave ($l = 0$) scattering between two identical fermionic atoms in the same hyperfine state (the lowest contribution is then a p -wave ($l = 1$) which vanishes as $\epsilon \rightarrow 0$), s -wave scattering occurs between different hyperfine states. We will concentrate our treatment to the latter case, and assume two identical fermions in hyperfine states labeled 1 and 2, respectively.

To compute the rate coefficient K , we need to average over the distribution of relative velocities in the system. The velocity distribution of each ensemble follows a Fermi distribution characterized by its temperature T and Fermi energy $E_F = k_B T_F$. Because of the setups in most experiments, we consider the atoms trapped in an harmonic potential. For large traps with frequencies ω_1, ω_2 , and ω_3 , the density of state for the hyperfine state i is given by $\rho(\vec{k}_i) = \hbar^3 k_i^3 / m^3 \omega_1 \omega_2 \omega_3$.

The Fermi energy E_F of the atoms in a particular hyperfine state is the energy of the highest occupied state in the harmonic potential at absolute zero and so is determined by the total number of atoms sharing the same hyperfine state. To have the same number of atoms in each hyperfine state provides two benefits: both group of atoms have the same Fermi energy, and the s -wave scattering rate is maximal. This requirement is not too stringent experimentally: if the sample is to be prepared from the atoms in a single hyperfine state by transferring $\sim 50\%$ of the atoms to another hyperfine state, then the maximal number difference between the two is determined by the degeneracy of the trap potential at the Fermi energy. E.g., for isotropic harmonic trap with the degeneracy of the m -th energy level $\sim m^2$ it follows $\Delta N/N \approx \cdot N^{-1/3}$. In what follows we assume that both hyperfine states have identical number of atoms so that their Fermi energies are identical as well.

The distribution of the relative momentum $\vec{\kappa}$ (normal-

ized to unity) is

$$\begin{aligned} g_{12}(\kappa) &= \int d^3 k_1 d^3 k_2 g(\vec{k}_1) g(\vec{k}_2) \delta(\vec{k}_1 - \vec{k}_2 - 2\vec{\kappa}), \\ &= \int d^3 k_2 g(\vec{k}_2) g(\vec{k}_2 + 2\vec{\kappa}), \end{aligned} \quad (4)$$

where $g(\vec{k}_i) \equiv \rho(\vec{k}_i) f_{\text{FD}}(\vec{k}_i, E_F, T) / N_i$. Here, the function $f_{\text{FD}}(\vec{k}_i, E_F, T) = \{1 + \exp[(E_{\vec{k}_i} - E_F) / k_B T]\}^{-1}$ is the Fermi-Dirac distribution with $E_{\vec{k}_i} = \hbar^2 k_i^2 / 2m$, and $N_i = \int d^3 k_i \rho(\vec{k}_i) f_{\text{FD}}(\vec{k}_i, E_F, T)$ is the number of fermions in the hyperfine state i . Note that $g_{12}(\kappa)$ depends on E_F and T , but not on the direction of $\vec{\kappa}$: the integration removes that dependence. In Fig. 2, we illustrate the distribution g_{12} in term of the relative energy ϵ for various temperatures and compare it with the corresponding Maxwell-Boltzmann (MB) distributions. As the temperature drops under T_F , the difference between the two types of distribution becomes more apparent; as the system becomes more degenerate, the g_{12} distribution spreads over a larger range of energies (when compared to MB distributions). As T approaches zero, g_{12} is entirely contained between $\epsilon = 0$ and $2E_F$. As opposed to the single particle distribution $g(E)$ (see inset), which is contained between $E = 0$ and E_F at zero- T and decreases sharply to zero at E_F , g_{12} goes to zero more gradually. In fact, for the case of free particles, one can show that $g_{12}(\epsilon)$ is a triangle with values 1 at $\epsilon = 0$ and 0 at $\epsilon = 2E_F$, while $g(E)$ is the standard step function between $E = 0$ and E_F .

We want to use 2-photon scattering to probe the relative velocity (or energy) distribution and infer the temperature of the system. At ultra-cold temperatures, Eq.(1) becomes $K = (\pi\hbar/2m) \int d^3 \kappa g_{12}(\kappa) |S_0|^2 / \kappa$, which can be rewritten in terms of ϵ as

$$K(T, L_1, L_2) = \frac{4\pi^2}{\hbar} \int_0^{\infty} d\epsilon g_{12}(\epsilon) |S_0(\epsilon, L_1, L_2)|^2. \quad (5)$$

Besides T and E_F , K depends on the detunings δ_1 and δ_2 and the Rabi frequencies Ω_1 and Ω_2 . Because of the important variation of $|S_0|^2$ with respect to δ_2 , lineshapes obtained as a function of δ_2 contain precious information about the degenerate Fermi gas. As T is reduced, the distribution g_{12} becomes more sharply defined for ϵ between 0 and $2E_F$, and by scanning δ_2 for nearby values, the large variations in the integrand of Eq.(5) will probe g_{12} .

We computed lineshapes for realistic systems. The Fermi energies E_F reached in today's experiments are in the range of few μK . In addition to this experimental constraint, one needs to be detuned far enough from resonance to not populate the level v_1 , with typical detunings $\delta_1 \sim 150$ MHz (7.2 mK) [14]. The lifetime of most levels v_1 is about 10-20 nsec, giving $\gamma_1 \sim 16 - 32$ MHz (0.76-0.38 mK) Finally, one needs intensities large enough to drive the transition, but not too large to heat the system (through broadening). Typical values for high lying

states v_1 at 500 GHz below the asymptote are $\Omega_1 = 100$ kHz (4.8 μ K) and $\Omega_2 \sim 2$ -3 MHz (96-144 μ K). Under these conditions, we have $\delta_1 \gg h\Omega_2$. With large δ_1 , Δ_+ will also be large, and the only way to get a peak of $|S|^2$ with $\epsilon \sim E_F$ will come from Δ_- : hence, we must have $\delta_2 \sim E_F$ as well. Then, $\delta_1 \gg h\Omega_2 \gg \delta_2$ and we will have peaks at $\Delta_- \sim \delta_2 - h^2\Omega_2^2/\delta_1$ and $\Delta_+ \sim \delta_1 + h^2\Omega_2^2/\delta_1$, as well as a minimum at $\epsilon = \delta_2$.

III. RESULTS AND DISCUSSION

We obtained lineshapes for various temperatures by varying δ_2 in (5). We selected parameters consistent with the case of ${}^6\text{Li}$ (although similar results can be obtained for other species): $E_F = 1$ μ K, $\delta_1 = 7$ mK, $\gamma_1 = 0.76$ mK and $h\Omega_2 = 100$ μ K. The remaining parameters lead to a multiplicative constant in K that can be factored out for all lineshapes. We show representative lineshapes normalized to unity (in arbitrary units) in Fig. 3; as T is lowered below T_F , the peak becomes narrower and sharper. Many other features can be identified on those lineshapes. As δ_2 grows, K reaches a minimum value K_{\min} , increases rapidly to its maximum value K_{\max} , and then decreases more slowly to a ‘‘background’’ value K_{bg} . In addition, inflection points on both sides of the peak can be identified. All these features can be extracted from the lineshapes, and could be used to extract temperature. For example, one could take the ratio $[K_{\max} - K_{\text{bg}}]/[K_{\min} - K_{\text{bg}}]$ of a given lineshape, in principle removing the multiplicative constant in K . However, this ratio varies very little for $T/T_F \sim 0.5$ and below. Besides the effect of a background signal/noise would also affect/reduce the sensitivity of the temperature determination. One could also map the location (i.e. the value of δ_2) of these features as a function of T , but again, their variations are small below say $T/T_F \sim 0.1$.

Alternative features, such as ratios of the derivatives at the inflection points (on each side of the main peak) could be used. In this case, the background would not play any role, nor the multiplicative constant in K . A simple measure incorporating both criteria is the ratio of the curvature of the signal at the peak value and its height as defined from the minimum value of K (see inset in Fig. 3), i.e.

$$C \equiv -\frac{K''(\delta_2^{\max})}{K_{\max} - K_{\min}} E_F^2. \quad (6)$$

While finding the second derivative of a lineshape with respect to δ_2 may be challenging in general, at the local peak maximum this should not be a problem as the first derivative there is zero.

Because of the rapid increase of K from its minimum value to its peak value, only a small range of δ_2 needs to be scanned (as compared to the ratio of the derivatives at the inflection points): for $E_F \sim 1$ μ K, scans with kHz precision are required. In Fig. 4, we show C as a function of T/T_F : it decreases monotonically with

T , and even at $T/T_F \sim 0.05$, its variation is noticeable. So, by measuring three features on the lineshape, namely its minimum, maximum, and the curvature at the maximum, one can evaluate C and determine the temperature of the degenerate Fermi sample by reading it from Fig. 4. Although the exact values of C depend on other parameters (γ_1 , δ_1 , and Ω_2), its general shape follows the example shown in Fig. 4. For illustration purposes, we also include two other curves (corresponding to other sets of δ_1 and Ω_2). The curve with the largest variations at low T/T_F is found when we have $\delta_1 \gg h\Omega_2 \gg \delta_2$ with a factor of 100 between each parameter.

The lineshapes shown in Fig. 3 are not very sensitive to small variations in γ_1 , δ_1 or Ω_2 : variations of few % give very similar curves. Of these parameters, γ_1 cannot be varied experimentally, except by changing the intermediate molecular level E_{b1} . However, for most atoms with Fermi species considered in today's experiments, i.e., alkali metals, γ_1 varies little with E_{b1} (e.g., for ${}^6\text{Li}_2$ in the triplet excited state, γ_1 varies from ~ 11.7 MHz down to 3.2 MHz (or 0.56 mK to 0.16 mK). However, systems with even smaller γ_1 (about 1-10 μ K) would offer the possibility of measuring the velocity distribution g_{12} directly by scanning δ_2 . In fact, $|S|^2$ then becomes proportional to the delta-function $\delta(\epsilon - \delta_2)$. The extremely small variations in g_{12} as $T \rightarrow 0$ could possibly be detected. Another possibility to enhance the sensitivity of this type of measurement could be realized using Feshbach resonances: a sharp increase in the integrand of Eq.(5) at $\epsilon \sim \epsilon_{\text{res}}$, where ϵ_{res} is the resonant relative energy, would emphasize the corresponding region of the velocity distribution. By positioning the resonance appropriately (e.g., via external magnetic fields), strong contribution of regions of g_{12} where small variations occur as $T \rightarrow 0$ could be obtained, hence more precise information could be extracted from the lineshapes. Notice that p -wave Feshbach resonances [15] could be used to enhance p -wave scattering in a single-fermion population.

IV. CONCLUSION

We have shown that the lineshapes obtained using a two-photon Raman probe can yield very precise determination of the temperature in degenerate Fermi gases. One of the key advantage of this approach, beside its non-destructive nature, is the extremely low temperatures measurable: in the example considered here, as low as $\sim 0.05T_F$. Although we have illustrated this two-color scheme for identical fermions in two different internal states with equal populations, this method can be made much more flexible. For example, if the populations are very different, the g_{12} distribution may exhibit sharper structures that could be used advantageously. The enhancement due to Feshbach resonances could also help probing chosen regions of g_{12} , and extend the method to samples of identical fermion in a single internal state, by using p -wave Feshbach resonances. Finally, when the

interaction between the fermions is attractive such as for ${}^6\text{Li}$, Cooper pairs may form. Photoassociation of a Cooper pair should demand less energy than the photoassociation of the two fermions produced by breaking either one or two Cooper pairs [16]. These processes should contribute additional features on top of the sim-

ple lineshapes, their locations and magnitudes probing the energy gap and the number of Cooper pairs.

We thank R.G. Hulet and M. Modugno for helpful discussions. This work was supported by the National Science Foundation Grant PHY-0140290 and by the University of Connecticut Research Foundation.

-
- [1] F. Dalfovo and S. Stringari, *Phys. Rev. A* **53**, 2477 (1996).
- [2] B. DeMarco and D.S. Jin, *Science* **285**, 1703 (1999).
- [3] A. Truscott, K. Strecker, W. McAlexander, G. Partridge, and R. Hulet, *Science* **291**, 2570 (2001).
- [4] M. Holland et al., *Phys. Rev. Lett.* **87**, 120406 (2001); J.N. Milstein, S.J.J.M.F. Kokkelmans, and M.J. Holland, *Phys. Rev. A* **66**, 043604 (2002).
- [5] K.M. O'Hara et al., *Science* **298**, 2179 (2002).
- [6] M.E. Gehm et al., arXiv:cond-mat/0212499 (2002).
- [7] G. Ferrari, *Phys. Rev. A* **59**, R4125 (1999).
- [8] G. Ferrari, M. Inguscio, W. Jastrzebski, G. Modugno, G. Roati, and A. Simoni, *Phys. Rev. Lett.* **89**, 053202 (2002).
- [9] H. Hu, X.-J. Liu, and M. Modugno, E-Print No. cond-mat/0301182 (2003); G. Modugno et al., *Science* **297**, 2240 (2002).
- [10] G. Modugno (private communication).
- [11] E. Timmermans and R. Côté, *Phys. Rev. Lett.* **80**, 3419 (1998); A.P. Chikkatur et al., *Phys. Rev. Lett.* **85**, 483 (2000).
- [12] R. Wynar et al., *Science* **287**, 1016 (2000); J.M. Gerton, D. Strekalov, I. Prodan, and R.G. Hulet, *Nature* **408**, 692 (2000); C. McKenzie et al., *Phys. Rev. Lett.* **88**, 120403 (2002).
- [13] J. Bohn and P. Julienne, *Phys. Rev. A* **54**, R4637 (1996).
- [14] R.G. Hulet (private communication).
- [15] C.A. Regal et al. arXiv:cond-mat/0209071 (2002).
- [16] P. Törmä and P. Zoller, *Phys. Rev. Lett.* **85**, 487 (2000).

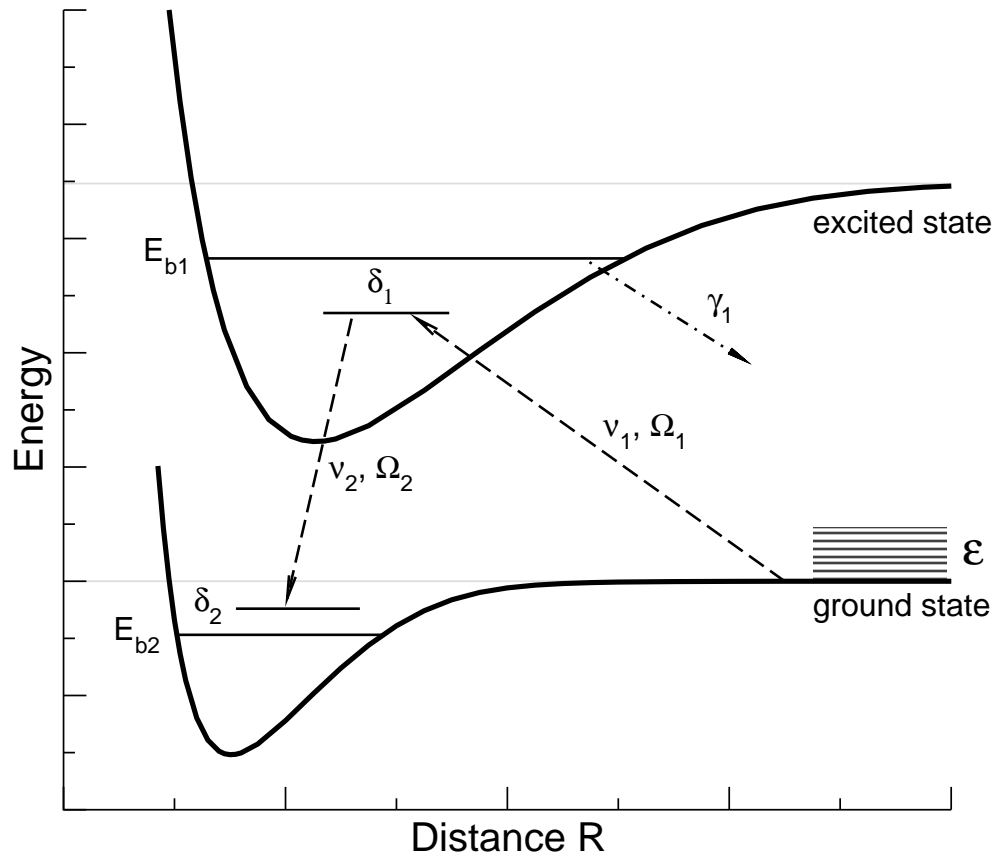


FIG. 1: Two-photon scheme. In this setup the detunings are $\delta_1 = E_{b1} - \nu_1 > 0$ and $\delta_2 = E_{b2} - \nu_1 + \nu_2 < 0$.

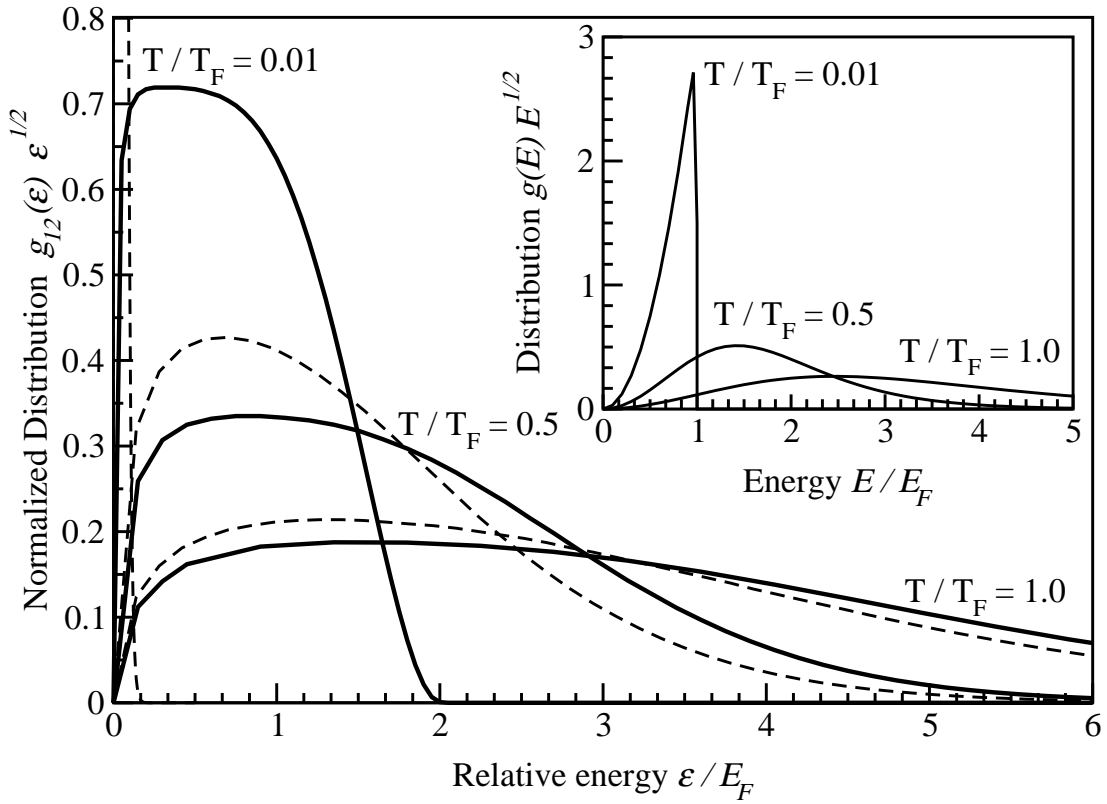


FIG. 2: Relative velocity distribution for various temperatures: $g_{l2}(\vec{\kappa})d^3\kappa = 2\pi(2\mu/\hbar^2)^{3/2}g_{l2}(\epsilon)\sqrt{\epsilon}d\epsilon$ (here, $g_{l2}(\epsilon)\sqrt{\epsilon}$ is normalized to unity). The effect of degeneracy becomes apparent when g_{l2} (solid lines) are compared to the corresponding Maxwell-Boltzmann distributions (dashed lines). The inset shows the corresponding single-particle distribution $g(E)\sqrt{E}$.

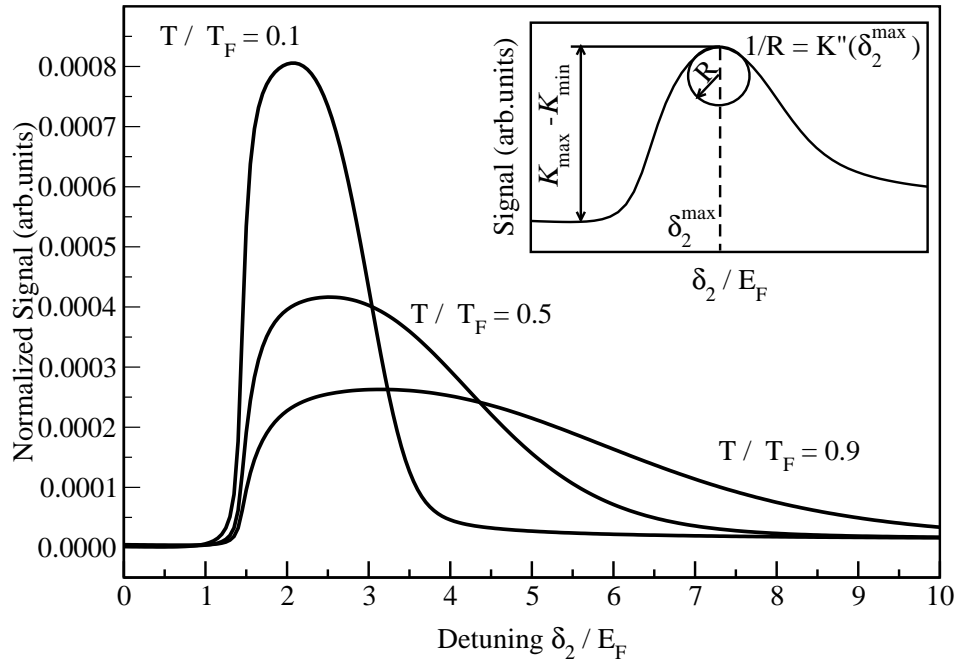


FIG. 3: Lineshapes as the functions of δ_2 for temperatures $T/T_F = 0.1, 0.5,$ and 0.9 , with $\gamma_1 = 3$ mK, $\delta_1 = 0.56$ mK, and $\Omega_2 = 100$ μ K. The definitions of K'' , K_{max} , K_{min} , and δ_2^{max} are illustrated in the inset.

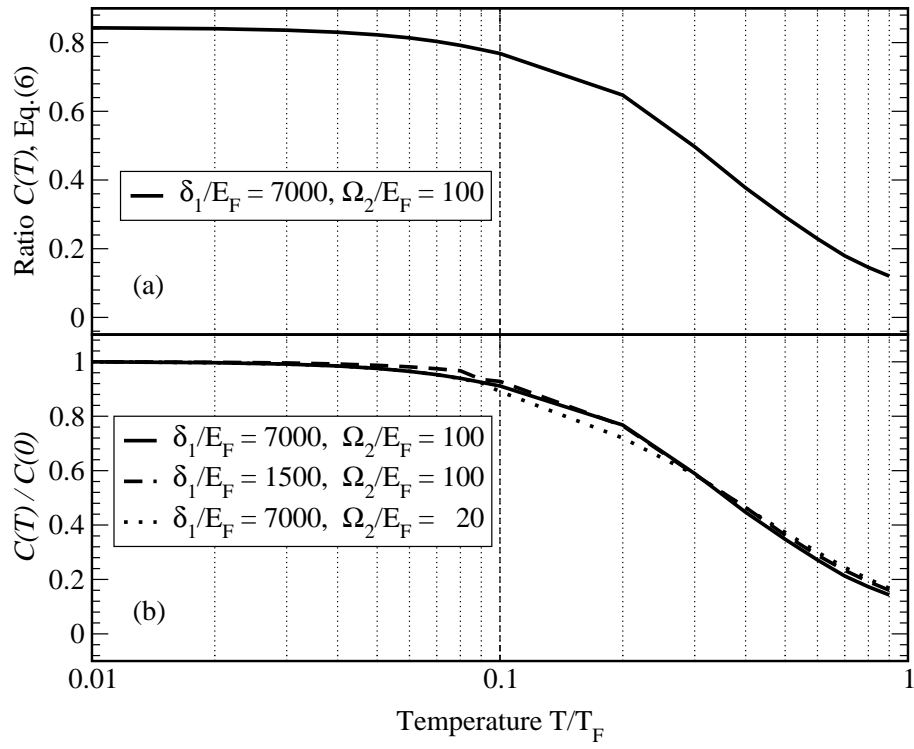


FIG. 4: Ratio C from Eq.(6) as a function of T/T_F . The sensitivity of C on other parameters is also illustrated by two other cases (dashed lines).